

Proposed Multiband Fractal Monopole Antenna for WLAN and WiMax Applications

Sonali Kumari^{1, *}, Yogendra K. Awasthi¹, and Dipali Bansal²

Abstract—A multiband fractal monopole antenna has been developed for wireless applications. A triangular monopole antenna is considered for this design to achieve the requirement of WLAN and WiMax. Annular rings are etched out from the basic antenna using the fractal concept. To increase its electrical length, notches are introduced at the edges. The volume of an antenna is $54 \times 57 \times 1.6 \text{ mm}^3$. Various changes in the ground plane have been done to get the optimum result. The frequency bands at which the antenna resonates are 3.5 GHz, 5.35 GHz, and 6.1 GHz. These bands are best suitable for the WiMax (3.5 GHz) and wireless local area network (5.35 and 6.1 GHz) applications. The simulated and experimental results show a good match.

1. INTRODUCTION

Monopole, as the word suggests, is a “radio aerial or pylon consisting of single pole or rod”. It has an omnidirectional radiation pattern, which radiates in all directions perpendicular to the antenna. The current demand for advanced technology is to develop a compact, space-friendly antenna with low cost. Different wireless communication applications require different frequency ranges such as W-LAN (2.4 GHz–2.484 GHz and 5.15 GHz–5.35 GHz/5.75 GHz–5.825 GHz), Wi-Max region (2.5 GHz–2.69 GHz, 3.4 GHz–3.69 GHz and 5.25 GHz–5.85 GHz), Wi-Fi region (2.4 GHz–2.484 GHz and 5.15 GHz–5.35 GHz), and RFID (2.45 GHz–5.8 GHz). Monopole antenna can be single-band or multiband. Here in this paper, the design of a monopole multiband antenna is proposed.

A multiband antenna is quite useful for wireless communication because a single antenna finds plethora of applications. Multiband can be achieved through different ways like DGS [1], slot cutting, reconfigurable antenna technique [2], and fractal Techniques [3–5]. In this paper, a fractal antenna with a notch and the technique are proposed. In 2014, Rajesh Kushwmar and Raghavan [6] proposed a trapezoidal ring quad-band fractal antenna. Fractal means ‘broken’. Fractal geometry design follows the repetition of a structure with a change in scale. Fractal geometry is well suited for designing multiband antennas as the similarity of a fractal with itself can be utilized to operate the antenna at several frequencies [7–9]. In Koch fractal [10], an inverted triangle with smaller dimensions is removed from the original triangle. In later designs, the triangular etching is replaced by a circle [11]. Several other modifications in the Sierpinski structure have been observed afterward. The circle has been replaced by an annular ring to get better results [12]. Several designs of antenna are reported with a change in the ground plane which gives resonance at desired frequencies [13, 14]. In the last few years, various researchers have been working on triangular slot, reconfigurable feeding, and L-band fractal antenna [15–17]. Various other works have been reported on UWB diversity antenna with two inverted L-shaped slots used for isolation [18]. A dual band-notched antenna has been used with L-slit as a filter [19]. Further, a CP gap coupled technique has been proposed for wideband antenna [20–22]. Band notches

Received 15 November 2022, Accepted 14 December 2022, Scheduled 19 December 2022

* Corresponding author: Sonali Kumari (sinha.sonali08@gmail.com).

¹ Manav Rachna International Institute of Research and Studies, Faridabad, India. ² G.B. Pant, DSEU, Okhla-1 Campus, New Delhi, India.

have been used for isolation. The above-reported antennas have complex structures with low gain. The present work reports a multiband antenna with good gain that satisfies the demand for modern-day wireless communication.

In this paper, the design proposed for the antenna is suitable for multiband operation. Here a basic Sierpinski structure (triangular-shaped) is modified to the annular ring. Initially, a triangular patch is designed, and an annular ring is etched out from the structure. Though the size has been reduced, the S_{11} response is not very satisfying. To rectify this problem notches are introduced in the structure. Notches are cut at two equal sides of an isosceles triangle. The cuts are done in such a way that they do not touch the annular ring. Various changes in the size of the notch have been done for better results. The resonant frequency is reduced as a result. Various notches have been cut in the structure to increase the electrical length to get the desired frequency range, and then various parametric changes in the ground plane have been done to obtain better results. Cutting slots to change the ground plane results in performance upgradation of the antenna.

The organization of the paper is as follows. Section 2 includes an overview of the proposed antenna design and its geometry descriptions. Section 3 includes the simulation results and parametric variations. Section 4 describes the results, which include simulated as well as experimental results. Section 5 explains the conclusion.

2. GEOMETRY OF ANTENNA DESIGN PROPOSED

An FR4 substrate has been taken for antenna designing with a dielectric constant, ϵ_r of 4.4, and loss tangent $\tan \delta = 0.025$. The proposed antenna is fed by using a microstrip line, and a lumped port has been assigned for excitation. The triangular monopole design is shown in antenna 1. By using the cavity model theorem with perfect magnetic walls, the equations for the various modes f_{mn} can be given [23, 24].

$$f_{mn} = f_{10} (m^2 + mn + n^2)^{1/2} \quad (1)$$

where,

$$f_{10} = \frac{2c}{3a\sqrt{\epsilon_r}} \quad (2)$$

and $f_{mn} = f_r$,

$$f_r = \frac{2c(m^2 + mn + n^2)^{1/2}}{3a\sqrt{\epsilon_r}} \quad (3)$$

so, the expression for the lowest order resonant frequency is

$$f_r = \frac{2c}{3a\sqrt{\epsilon_r}} \quad (4)$$

where

- f_r = resonant frequency
- a = side length of the triangular patch
- ϵ_r = dielectric constant of the substrate
- c = free space light velocity

Dimensions are calculated on the basis of the length and width of the given formula of triangular patch [25]. On the lower half of the substrate, the ground plane has been placed. As the size of the triangle is reduced, frequency shifts towards the higher side. To solve this problem, notches are added. By adding notches, electrical length is increased, due to which the resonant frequency shifts to the lower side, and hence more resonant frequencies are obtained. Various trials for optimization have been attempted so that it does not disturb the annular ring and gives the desired results. N_1 , N_2 , N_3 , and N_4 are four positions of notches. Notches have been added at both sides of an isosceles triangle. The widths of all the notches are the same (1 mm), as shown in Design 4. Various changes have been made on a ground plane to get better results with better return loss at all the resonant frequencies. Design 5 shows the four rectangles of $(6 \times 3) \text{ mm}^2$ that have been removed from the ground plane. In Design 6, eight

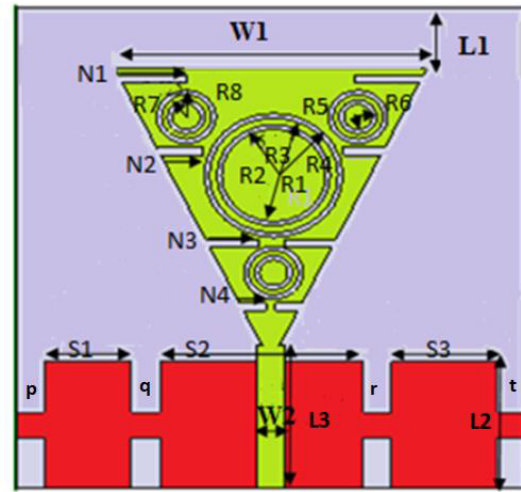
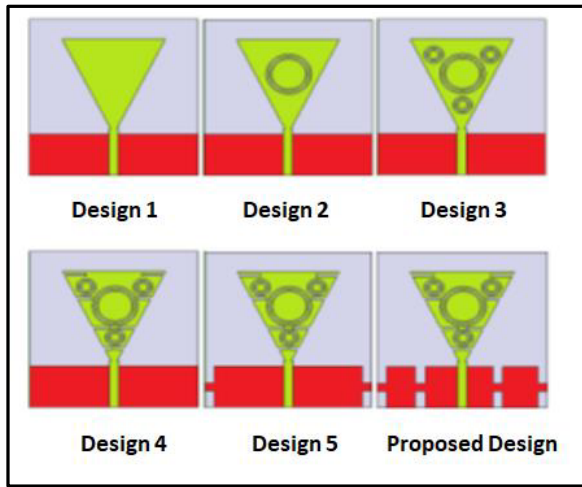


Figure 1. Design steps of antenna structure from simple triangular patch to final structure (Design 1 to proposed design).

Figure 2. Final proposed structure.

Table 1. Dimensions of antenna design proposed.

Parameters	L	$L1$	$L2$	W	$S1$	$S2$	$S3$	$N1$	$N2$	$N3$
Value (mm)	57	22.3	15	54	9.25	21.5	11.25	7.2	4.8	5.7
Parameter	$N4$	$R1$	$R2$	$R3$	$R4$	$R5$	$R6$	$R7$	$R8$	
Value (mm)	3.5	5.5	6	6.825	7	1.5	2	2.65	3.15	

rectangles have been removed from the structure, four rectangles at the four corners and four rectangles in the middle, as shown in Fig. 1. All the rectangles which have been removed from the ground plane are equal in dimension. The proposed design is the final structure with eight slot cuts. Fig. 1 shows the stage-wise development, from a simple triangular patch to get the final proposed structure. Fig. 2 is the final structure, and all the dimensions are given in Table 1.

3. SIMULATION OF PROPOSED DESIGN AND DISCUSSION ON PARAMETRIC VARIATION

3.1. Simulation Analysis

The simulated results for S_{11} for Design 1 to Design 6 are given in Fig. 3. It gives a comparative result of the return losses of all the structures. Design 1 is a simple triangular monopole antenna, which gives return loss at 7.3 GHz, and then annular rings are etched out from the triangular monopole. When it simulates, it gives maximum return loss at 3.85 GHz and 7.3 GHz. To increase the electrical length notches are cut out as shown in Design 3, which gives good matching at 3.65 GHz and 5.8 GHz. If these S_{11} results (Design 3) are compared with the simulation results of the previous Design 2, it is found that there is a shift in the frequency towards the lower-side as we progress from Design 1 to Design 3.

Then various changes have been done in the ground plane, so that better impedance matching is achieved. In Design 5, four rectangular slots have been cut from the ground plane as depicted in Fig. 1. While moving from Design 5 to Proposed Design, various changes in the ground plane have been tried. The first four rectangular slots are at four corners and then four rectangular-slots in the middle of the ground plane. Comparison results of all the steps from Design 1 to Proposed Design are listed in Table 2.

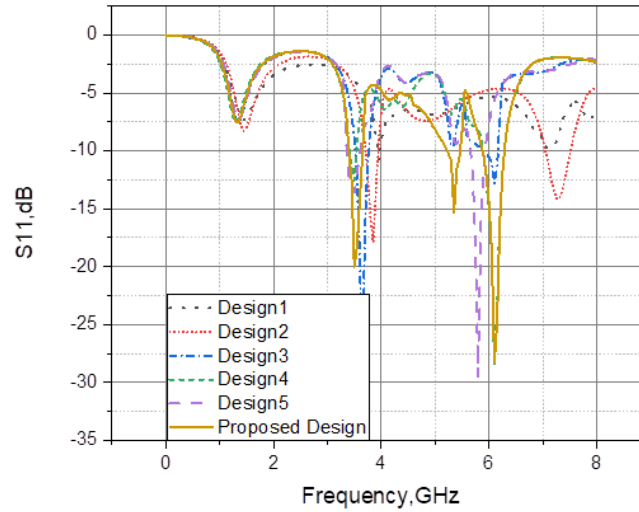


Figure 3. Comparative simulation results of various antenna design.

Table 2. Comparison of various antenna designs.

Antenna Design	Frequency Band (GHz)	Maximum Return loss (dB)	Corresponding Resonant frequency (GHz)	Bandwidth (MHz)
Design 1	3.95	-10.82	3.95	-
Design 2	3.75–3.9	-17.88	3.85	150
Design 3	3.55–3.75	-30.71	3.65	200
	5.9–6.15	-12.81	6.1	250
Design 4	3.45–3.5	-12.55	3.5	50
	5.9–6.25	-28.45	6.1	350
Design 5	3.4–3.6	-13.60	3.5	200
	5.7–5.9	-29.48	5.8	200
Proposed Design	3.4–3.75	-28.22	3.5	250
	4.75–5.5	-22.30	5.35	200
	5.95–6.55	-33.30	6.1	350

3.2. Phenomenon of Current Distribution

The distribution of current on the antenna surface is shown in Fig. 4. Fig. 4(a) shows the maximum current at the feeding strip and radiating element of triangle patch, so the first resonance at 3.5 GHz arises due to the triangular patch with the annular ring while in Fig. 4(b) the maximum current is due to the notch present in a triangle. Due to this notch, there is the resonance at 5.35 GHz and in the third figure maximum current due to the slot cut in ground and annular ring in triangular patch, so the resonance is coming due to change in the ground plane. Therefore, the three resonances which are below 10 dB are due to annular cut in triangular patch, notches, and change in the ground plane.

3.3. Parametric Validation

To get the best results, parametric variation was performed, changing only one parameter at a time.

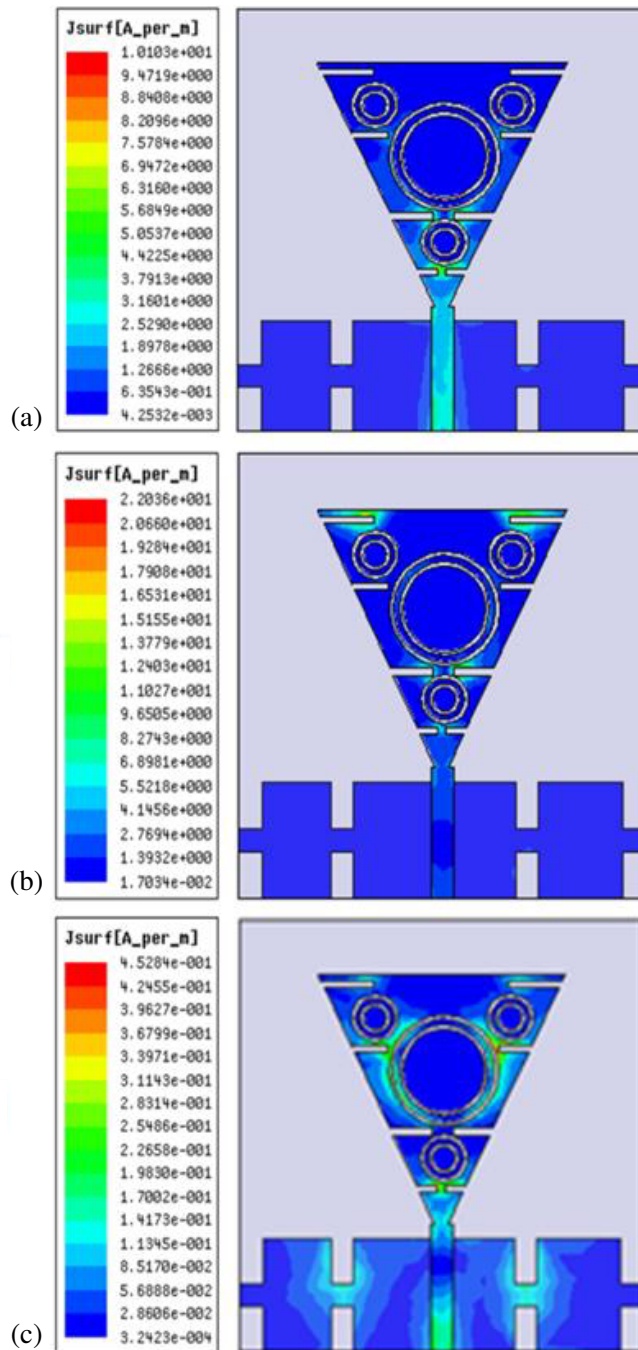


Figure 4. Simulated current distribution of the final proposed structure at (a) 3.5, (b) 5.35 and (c) 6.1 GHz.

3.3.1. Parametric Variation in the Slot Width

Parametric change in slot width has been performed to get the best result. P & q & r & t are the slot widths removed from the ground. Simulation results of parametric variation are given in Figs. 5, 6, 7, and 8, respectively, for slot widths p , q , r , and t . Tables 3, 4, 5, and 6 provide the parametric variations of p , q , r , and t , respectively.

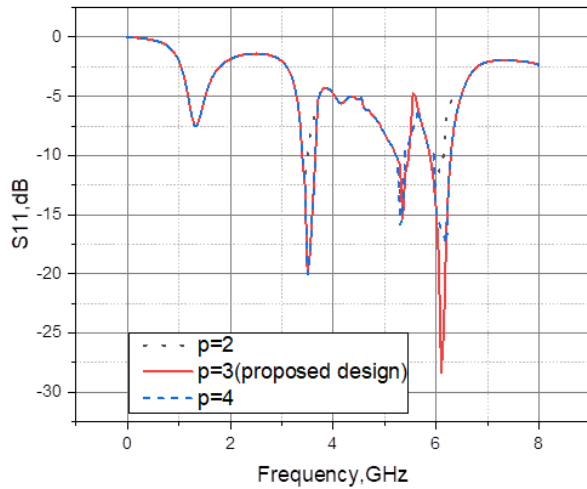


Figure 5. Simulation results of parametric variation in the slot width ' p '.

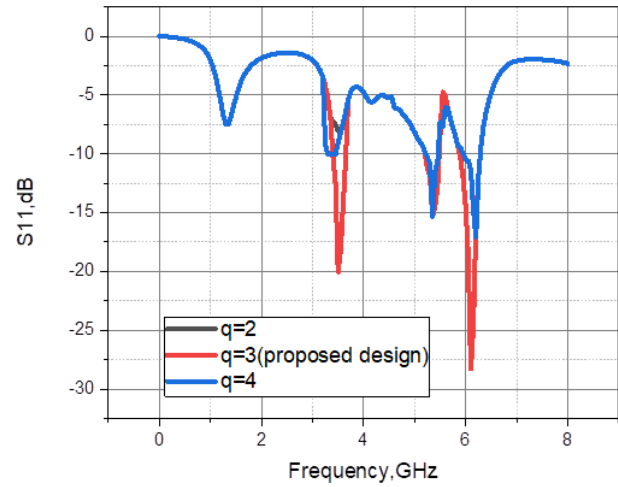


Figure 6. Simulation results of parametric variation in the slot width ' q '.

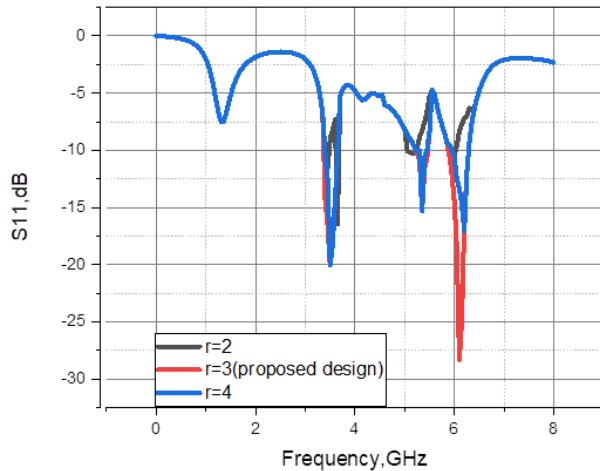


Figure 7. Simulation results of parametric variation in the slot width ' r '.

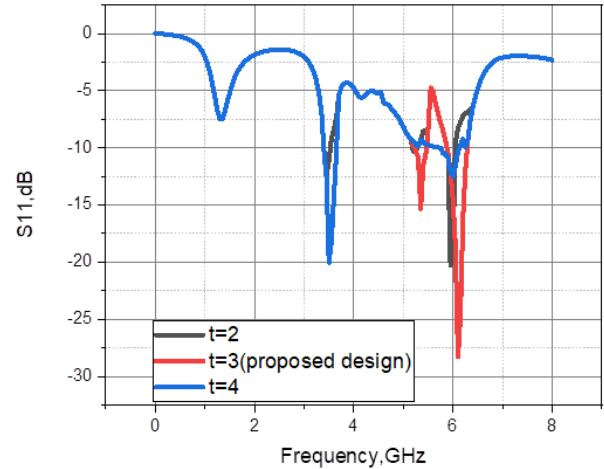


Figure 8. Simulation results of parametric variation in the slot width ' t '.

4. RESULTS AND DISCUSSION

After detailed analysis of parametric variations made, the proposed design is confirmed for fabrication.

The antenna design was performed using Ansys HFSS software 13, and its characteristics were measured by a vector network analyzer (Model MS2038C). The fabricated structure is depicted in Figs. 9(a) and 9(b). Antenna Testing is done in an anechoic chamber. The comparative S_{11} results (measured and simulated) are shown in Fig. 10. There is a slight variation in measured and simulated results of return loss, which is quite possible and also permissible. Comparative gain results (measured and simulated) are shown in Fig. 11. Fig. 12 depicts the co-polarization and cross-polarization of the simulated & measured radiation patterns of the two major cutting E and H planes. Omnidirectional patterns are obtained at E or H planes due to the monopole antenna.

The gain versus frequency graph is shown in Fig. 11. Here peak gain is observed as 5.9 dB at 6.1 GHz. The rest of the frequencies are 3.5 GHz and 5.35 GHz, and also gain is coming as 3.9 dB and 3 dB, respectively. The final proposed structure with notches on the triangular monopole and slots cut in

Table 3. Comparison of S_{11} results due to parametric changes of ' p '.

Slot width	Frequency Band (GHz)	Max. Return loss (dB)	Resonance Frequency (GHz)	Bandwidth (MHz)
$P = 2$	3.4–3.5	–12.03	3.45	100
	5.25–5.45	–15.30	5.35	200
	5.9–6.15	–12.30	5.95	250
$P = 3$ (Proposed Design)	3.4–3.65	–20.03	3.5	250
	5.25–5.45	–15.30	5.35	200
	5.9–6.25	–28.30	6.1	350
$P = 4$	3.4–3.65	–20.03	3.5	250
	5.25–5.35	–13.30	5.30	100
	6.0–6.25	–17.05	6.2	250

Table 4. Comparison of S_{11} results due to parametric changes of q .

Slot width	Frequency Band (GHz)	Max. Return loss (dB)	Resonance Frequency (GHz)	Bandwidth (MHz)
$q = 2$	5.25–5.45	–15.30	5.35	200
	5.9–6.25	–28.30	6.1	350
$q = 3$ (Proposed Design)	3.4–3.65	–20.03	3.5	25
	5.25–5.45	–15.30	5.35	20
	5.9–6.25	–28.30	6.1	35
$q = 4$	3.3–3.45	–10.03	3.4	150
	5.25–5.40	–15.30	5.35	150
	6.0–6.25	–17.05	6.2	250

Table 5. Comparison of S_{11} results due to parametric change of r .

Slot width	Frequency Band (GHz)	Max. Return loss (dB)	Resonance Frequency (GHz)	Bandwidth (MHz)
$r = 2$	3.4–3.5	–12.03	3.45	100
	5.05–5.25	–10.30	5.20	200
	5.9–6.25	–11.30	5.95	100
$r = 3$ (Proposed Design)	3.4–3.65	–20.03	3.5	250
	5.25–5.45	–15.30	5.35	200
	5.9–6.25	–28.30	6.1	350
$r = 4$	3.4–3.65	–20.03	3.5	250
	5.25–5.45	–15.30	5.35	200
	6.0–6.25	–17.05	6.2	250

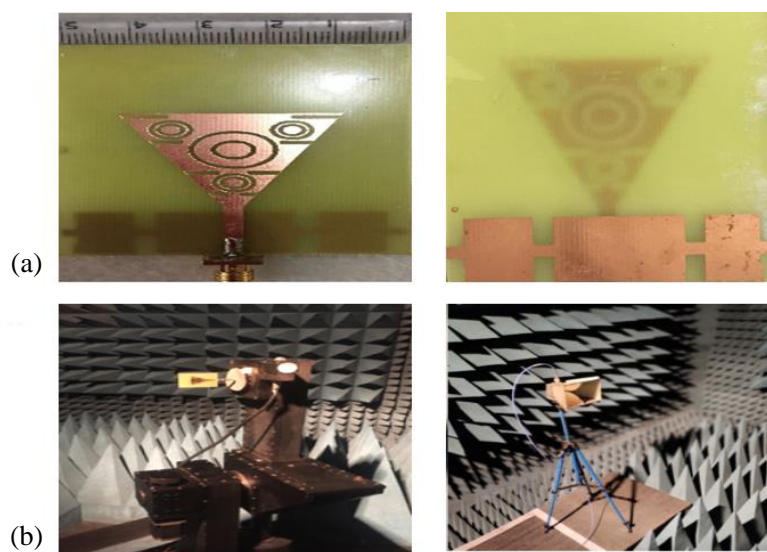
the ground-plane is fabricated on an FR4 substrate. Fabrication is done using micromachining. Table 7 shows the comparison of simulated & measured results. The designed antenna shows a decent radiation pattern for all the frequencies which is the response of an ideal monopole except for a slight distortion at 5.35 GHz. Table 8 shows the comparative result of the proposed structure with other similar designs.

Table 6. Comparison of S_{11} results due to parametric change of t .

Slot width	Frequency Band (GHz)	Max. Return loss (dB)	Resonance Frequency (GHz)	Bandwidth (MHz)
$t = 2$	3.4–3.5	−12.03	3.45	100
	5.05–5.25	−10.30	5.20	200
	5.9–6.0	−20.30	5.95	100
$t = 3$ (Proposed Design)	3.4–3.65	−20.03	3.5	250
	5.25–5.45	−15.30	5.35	200
	5.9–6.25	−28.30	6.1	350
$t = 4$	3.4–3.65	−20.03	3.5	250
	5.8–6.12	−12.05	6.0	320

Table 7. Return loss compared for simulated and measured values.

Readings	Frequency-band (GHz)	Resonant Frequency (GHz)	Maximum Return loss (dB)	Bandwidth (GHz)
Measured	3.4–3.75	3.55	−28.22	0.35
	4.75–5.5	5.35	−22.30	0.75
	5.95–6.55	6.1	−33.30	0.6
Simulated	3.4–3.65	3.5	−20.03	0.25
	5.25–5.45	5.35	−15.3	0.2
	5.9–6.25	6.1	−28.30	0.35

**Figure 9.** Proposed fabricated antenna structure. (a) Front & back side. (b) Antenna testing at anechoic chamber.

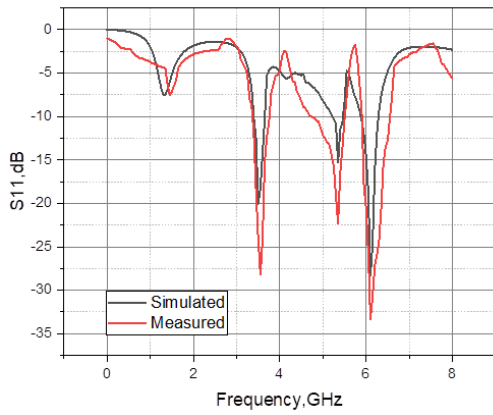


Figure 10. Comparative graph of experimental and simulated S_{11} of the final proposed design.

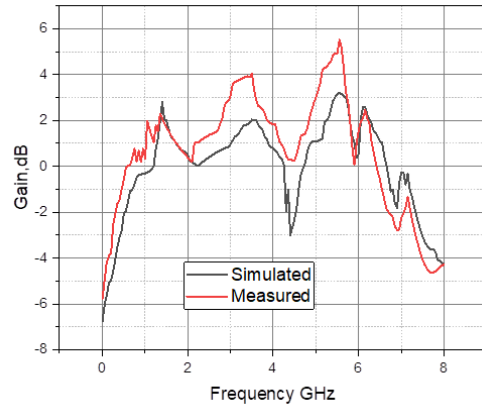


Figure 11. The gain vs. frequency plot of the proposed structure.

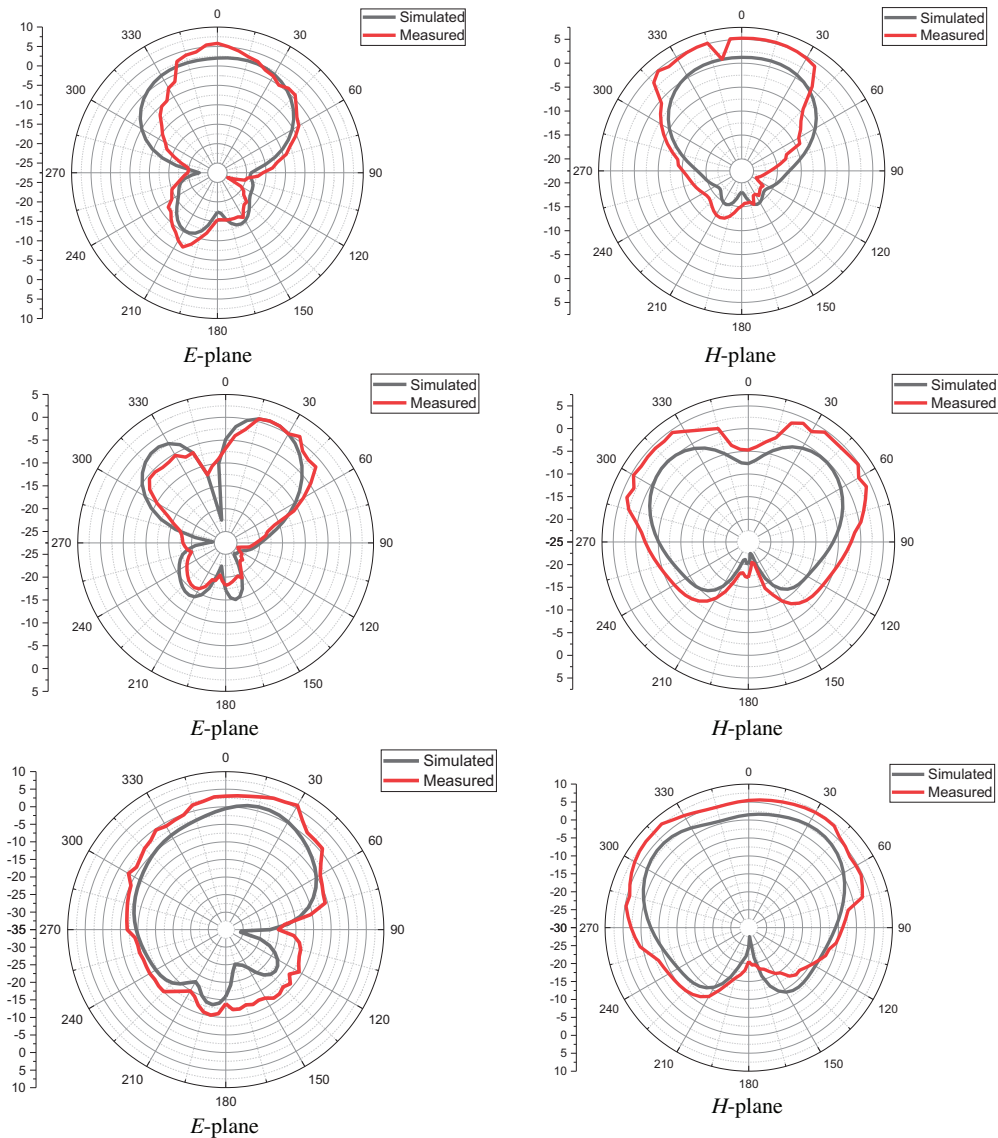


Figure 12. The radiation pattern of simulated and measured proposed antenna in E -plane and H -plane at 3.5, 5.35, and 6.1 GHz.

Table 8. Proposed design compared with existing similar designs.

References	Size of Antenna (mm ³)	Frequency Band (GHz)	Peak Gain (dB)
[15]	87.5 × 61 × 1.6	1.8–2.9, 3.4–4.6, 5–5.6	3.34
[16]	83.5 × 50.5 × 1.524	1.0–1.2	2.1
[17]	100 × 100 × 1.6	0.94–2.25	5.49
[10]	80 × 90 × 1.6	8.2, 12.4, 18	-
Proposed design	54 × 57 × 1.6	3.45–3.75, 4.75–5.5, 5.95–6.2	5.90

5. CONCLUSION

A fractal monopole antenna has been designed, and the complete analysis has been described in the article above. The final results of simulated and fabricated structures are in good agreement with each other. The proposed structure provides cost-effective solutions as it is reduced to 50% of its original size. The notch used in the triangular monopole accounts for the space-friendly size of the antenna as it has increased the electrical length. After making the parametric changes in the ground plane, the gain has also been enhanced. The proposed monopole multiband fractal antenna finds its applications in WiMAX for 3.5 GHz and WLAN for 5.35 GHz and 6.1 GHz.

REFERENCES

1. Ghaffar, A., W. A. Awan, N. Hussain, S. Ahmad, and X. J. Li, "A compact dual-band flexible antenna for applications at 900 and 2450 MHz," *Progress In Electromagnetics Research Letters*, Vol. 99, 83–91, 2021.
2. Mansoul, A. and M. L. Seddiki, "Multiband reconfigurable Bowtie slot antenna using switchable slot extensions for WiFi, WiMAX, and WLAN applications," *Microwave and Optical Technology Letters*, Vol. 60, No. 2, 413–418, 2018, <https://doi.org/10.1002/mop.30981>.
3. Anand, R. and P. Chawla, "Bandwidth optimization of a novel slotted fractal antenna using modified lightning attachment procedure optimization," *Smart Antennas*, 379–392, 2022, https://doi.org/10.1007/978-3-030-76636-8_28.
4. Anand, R. and P. Chawla, "Optimization of inscribed hexagonal fractal slotted microstrip antenna using modified lightning attachment procedure optimization," *International Journal of Microwave and Wireless Technologies*, Vol. 12, No. 6, 519–530, 2020, <https://doi.org/10.1017/s1759078720000148>.
5. Anand, R. and P. Chawla, "A novel dual-wideband inscribed hexagonal fractal slotted microstrip antenna for C- and X-band applications," *International Journal of RF and Microwave Computer-Aided Engineering*, Vol. 30, No. 9, 2020, <https://doi.org/10.1002/mmce.22277>.
6. Rajesh Kuswmar, V. and S. Raghavan, "Trapezoidal ring quad-band fractal antenna for WLAN/WiMAX applications," *Microwave and Optical Technology Letters*, Vol. 56, No. 11, 2545–2548, 2014.
7. Puente-Baliarda, C., J. Romeu, R. Pous, and A. Cardama, "On the behavior of the Sierpinski multiband fractal antenna," *IEEE Transactions on Antennas and Propagation*, Vol. 46, No. 4, 517–524, 1998.
8. Gianvittorio, J. and Y. Rahmat-Samii, "Fractal antennas: A novel antenna miniaturization technique, and applications," *IEEE Antennas and Propagation Magazine*, Vol. 44, No. 1, 20–36, 2002, doi: 10.1109/74.997888.
9. Wqrner, D. and S. Ganguly, "An overview of fractal antenna engineering research," *IEEE Antennas and Propagation Magazine*, Vol. 45, No. 1, 38–57, 2003, doi: 10.1109/map.2003.1189650.

10. Siddiqui, M. G., A. K. Saroj, Devesh, and J. Ansari, "Multi-band fractaled triangular microstrip antenna for wireless applications," *Progress In Electromagnetics Research M*, Vol. 65, 51–60, 2018.
11. Mehdipour, A., I. D. Rosca, A. Sebak, C. W. Trueman, and S. V. Hoa, "Full-composite fractal antenna using carbon nanotubes for multiband wireless applications," *IEEE Antennas and Wireless Propagation Letters*, Vol. 9, 891–894, 2010, doi: 10.1109/lawp.2010.2076342.
12. Kumari, S., S. Srivastava, and R. K. Lai, "Design of monopole fractal antenna using annular ring for RFID applications," *2015 International Conference on Soft Computing Techniques and Implementations (ICSCIT)*, 2015, doi: 10.1109/icseti.2015.7489579.
13. Ojaroudi, N. and N. Ghadimi, "Omnidirectional microstrip monopole antenna design for use in microwave imaging systems," *Microwave and Optical Technology Letters*, Vol. 57, No. 2, 395–401, 2014, doi: 10.1002/mop.28856.
14. Jalali, M. and T. Sedghi, "Very compact UWB CPW-fed fractal antenna using modified ground plane and unit cells," *Microwave and Optical Technology Letters*, Vol. 56, No. 4, 851–854, 2014, doi: 10.1002/mop.28194.
15. Wang, L., J. Yu, T. Xie, and K. Bi, "A novel multiband fractal antenna for wireless application," *International Journal of Antennas and Propagation*, 2021.
16. Kumar, M. M., A. Patnaik, and C. G. Christodoulou, "Design and testing of a multifrequency antenna with a reconfigurable feed," *IEEE Antennas and Wireless Propagation Letters*, Vol. 13, 730–733, 2014, <https://doi.org/10.1109/lawp.2014.2315433>.
17. Mukti, P. H., S. H. Wibowo, and E. Setijadi, "A compact wideband fractal-based planar antenna with meandered transmission line for L-band applications," *Progress In Electromagnetics Research C*, Vol. 61, 139–147, 2016.
18. Gautam, A. K., A. Saini, N. Agrawal, and N. Z. Rizvi, "Design of a compact protrudent-shaped ultra-wideband multiple-input-multiple-output/diversity antenna with band-rejection capability," *International Journal of RF and Microwave Computer-Aided Engineering*, Vol. 29, No. 9, 2019, doi: 10.1002/mmce.21829.
19. Chandel, R., A. K. Gautam, and K. Rambabu, "Tapered fed compact UWB MIMO-diversity antenna with dual band-notched characteristics," *IEEE Transactions on Antennas and Propagation*, Vol. 66, No. 4, 1677–1684, 2018, doi: 10.1109/tap.2018.2803134.
20. Verma, M. K., B. K. Kanaujia, J. P. Saini, and P. Saini, "A novel circularly polarized gap-coupled wideband antenna with DGS for X/Ku-band applications," *Electromagnetics*, Vol. 39, No. 3, 186–197, 2018.
21. Chandel, R. and A. Gautam, "Compact MIMO/diversity slot antenna for UWB applications with band-notched characteristics," *Electronics Letters*, Vol. 52, No. 5, 336–338, 2016.
22. Kumari, S., Y. K. Awasthi, and D. Bansal, "A miniaturized circularly polarized multiband antenna for Wi-MAX, C-band & X-band applications," *Progress In Electromagnetics Research C*, Vol. 125, 117–131, 2022.
23. Lee, K.-F., K.-M. Luk, and J. Dahele, "Characteristics of the equilateral triangular patch antenna," *IEEE Transactions on Antennas and Propagation*, Vol. 36, No. 11, 1510–1518, 1988, <https://doi.org/10.1109/8.9698>.
24. Verma, S., J. A. Ansari, and A. Singh, "Truncated equilateral triangular Microstrip antenna with and without superstrate," *Wireless Personal Communications*, Vol. 95, No. 2, 873–889, 2016, <https://doi.org/10.1007/s11277-016-3803-x>.
25. Balanis, C. A., *Antenna Theory: Analysis and Design*, John Wiley & Sons, Hoboken, NJ, 2012.